SIMULATION OF CONTINUOUS AND INTERRUPTED ROLLING PRACTICE OF HSLA STEEL

Warren W. Knudsen

A Thesis in the Faculty

of Engineering

Presented in Partial Fulfillment of the Requirements

for the Degree of Master of Engineering at

Concordia University

Montreal, Quebec.

March 1979

ABSTRACT

SIMULATION OF CONTINUOUS AND INTERRUPTED ROLLING PRACTICE OF HSLA STEEL

Warren W. Knudsen

Continuous and interrupted torsion tests were conducted between 800 and 1000° C at surface shear strain rates of 0.1, 1.0, and 10s^{-1} on HSLA steels. One set of tests simulated a hot reversing mill with hot coilers. The strain in each pass was held constant at 0.3 but the interval between passes alternated between 150 and 10 seconds. A second series of tests were conducted at strains of 2.5 and interruption time of 10 seconds to determine the effect on static restoration of dynamic recrystallization as opposed to that of dynamic recovery which is the preponderant mechanism at the low strains.

The static softening mechanisms operating during an interruption were determined from the fractional softening and by comparison of the stress level after the interruption with that produced by continuous deformation. The restoration mechanisms observed were static recovery, static recrystallization and grain growth. The amount of softening achieved depended upon the strain, strain rate, deformation temperature and length of interruption.

Acknowledgments

The author wishes to express his gratitude and deep appreciation to his research directors, Dr. H.J. McQueen and Dr. D.H. Hawkins. In addition, the author is grateful to Dr. J.J. Jonas, Dr. I. Weiss, and Gilles Canova for providing advise and experimental assistance during this investigation and to the SIDBEC-DOSCO STEEL COMPANY for providing the experimental materials.

TABLE OF CONTENTS

List of Figures

Page

Page

Page

List of Tables

CHAPTER 1

Introduction

Since their introduction in 1960, HSLA* steels have been used extensively as a structural material. The addition of small amounts of niobium and vanadium has the effect of increasing the yield strength of these steels. The predominate strengthening mechanism being a reduced ferrite grain size rather than precipitation of niobium or vanadium carbides. However, precipitation of these carbides makes the study of hot deformation of HSLA steels more complex as both recovery and recrystallization rates are affected differently by the presence of niobium or vanadium in solute form or as precipitates. Thus rolling schedules for such steels should take into account not only the kinetics of recovery and recrystallization but also those of precipitation and the interactions between the mechanisms. These can have significant effects since a retardation of dynamic recrystallization causes an increase in flow stress and a decrease in ductility.

* High strength low alloy

The torsion test has proven to be a useful tool for investigating the flow characteristics of metals during hot and cold working operations because it is able to produce high and constant strain rates. Also the problem of necking, encountered during tensile testing, and barrelling, encountered during compression testing, do not exist in torsion. In consequence, a torsion tester is capable of a sequence of tests which simulate a hot rolling operation which has a high total strain.

To simulate rolling schedules for an HSLA steel both continuous and interrupted torsion tests were conducted. In particular, deformations and interruption times were matched to the rolling schedule utilized at Contrecoeur, Quebec by SIDBEC-DOSCO on a reversing hot mill with hot coilers.

CHAPTER 2

Hot Working of HSLA Steels

Hot working has been simply defined as the deformation of a metal above its recrystallization temperature. However, this definition is not completely suitable because several softening mechanisms are operating during and between deformations, all of which contribute to the total softening (1-7). Therefore, the accepted definition of hot working is deformation at strain rates of 10^{-3} to 10^{3} s^{-1} which is imparted above 0.5 Tm where Tm is the melting temperature of the metal in degrees Kelvin (8).

2.1 Dynamic Softening Mechanisms

a) Dynamic Recovery

During deformation, dynamic recovery and dynamic recrystallization soften the metal and increase ductility. At low strains, dynamic recovery is the only softening mechanism operating in all metals, and continues as the sole mechanism at high strains in metals of high stacking

fault energy in which dislocations can easily move out of the slip plane.

As deformation proceeds, dislocations multiply and become entangled into a substructure within the grains (1,3,9). As deformation continues, the sub-boundaries increase in dislocation density until in the case of metals with a high stacking fault energy, a dynamic equilibrium is reached between dislocation generation and annihilation (1,10,11). When the subgrains reach the equilibrium condition, a steady state is established in which the flow stress remains constant (Fig. 2.1). These subgrains remain equiaxed even after true strains of 3 or 4 have been attained indicating that individual sub-boundaries are being formed and decomposed. The mechanism for unravelling of the substructure undoubtedly involves the unpinning of the attractive junctions (3,12).

The subgrains increase in size as the temperature of deformation increases or as the strain rate decreases (1). These larger subgrains contain fewer dislocations

and their boundaries also contain less dislocations. Along with the formation of a substructure, dynamic recovery also involves annihilation of dislocations in pairs.

b) Dynamic Recrystallization

If the dislocation density builds up to a critical level, dynamic recrystallization can occur (1,2,7,8); in other words, there is a critical strain for dynamic recrystallization. Dynamic recrystallization is generally observed in metals with low stacking fault energy whereas in metals with high stacking fault energy it seldom occurs because dynamic recovery produces a very low dislocation density (1). Since face-centered cubic structures, such as copper, nickel (4,17), austenitic stainless steels (5,15), nickel based superalloys (6), and plain carbon steels (when worked in the austenitic region) (15), have a low stacking fault energy, dynamic recrystallization is observed operating at high strains. HSLA steels above 750° C are face-centered-cubic and exhibit dynamic recrystallization under appropriate deformation conditions.

At lower strain rates, nucleation of dynamic recrystallization appears to occur by bulging of an existing grain boundary (17). At higher strain rates, nuclei develop throughout the grain when misorientation between the subgrains reaches approximately ten degrees (1,7). The grains which orginate from these nuclei are being deformed as they grow. At low strain rates (below those commonly used in hot working), the recrystallization goes to completion before the dislocation density builds up to a condition at which recrystallization is again nucleated. At higher strain rates, however, the dislocation densities at the center of the recrystallized grains increase sufficiently that nucleation occurs again before recrystallization is complete. Thus, throughout the grain, different degrees of deformation are present - from zero deformation to strains high enough to cause recrystallization. This distribution of dislocation substructures maintains a steady state flow stress between the yield stress of statically recrystallized material and the peak stress (Fig. 2.2)(1). Dynamic recrystallization involves the elimination of large numbers of dislocations by migrating grain boundaries. It should be

noted that during dynamic recrystallization, dynamic recovery continues to operate in the regions where deformation is causing dislocations to accumulate.

2.2 High Temperature Stress - Strain Curves

The stress - strain curves obtained during deformation of a metal are influenced by the softening mechanism operating. For a material which only dynamically recovers, the flow stress increases to a plateau and ideally maintains this steady state (1,2) (Fig. 2.1). However, in many cases, other softening mechanisms reduce the flow stress after the plateau has been reached. These mechanisms include adiabatic heating, precipitation coarsening, etc.

The flow curve obtained during dynamic recrystallization increases to a peak in the work hardening region (Fig. 2.2). This peak is associated with the initiation of nucleation and is followed by a decrease in stress (work softening region), to a value still considerably higher than the yield stress (1,2).

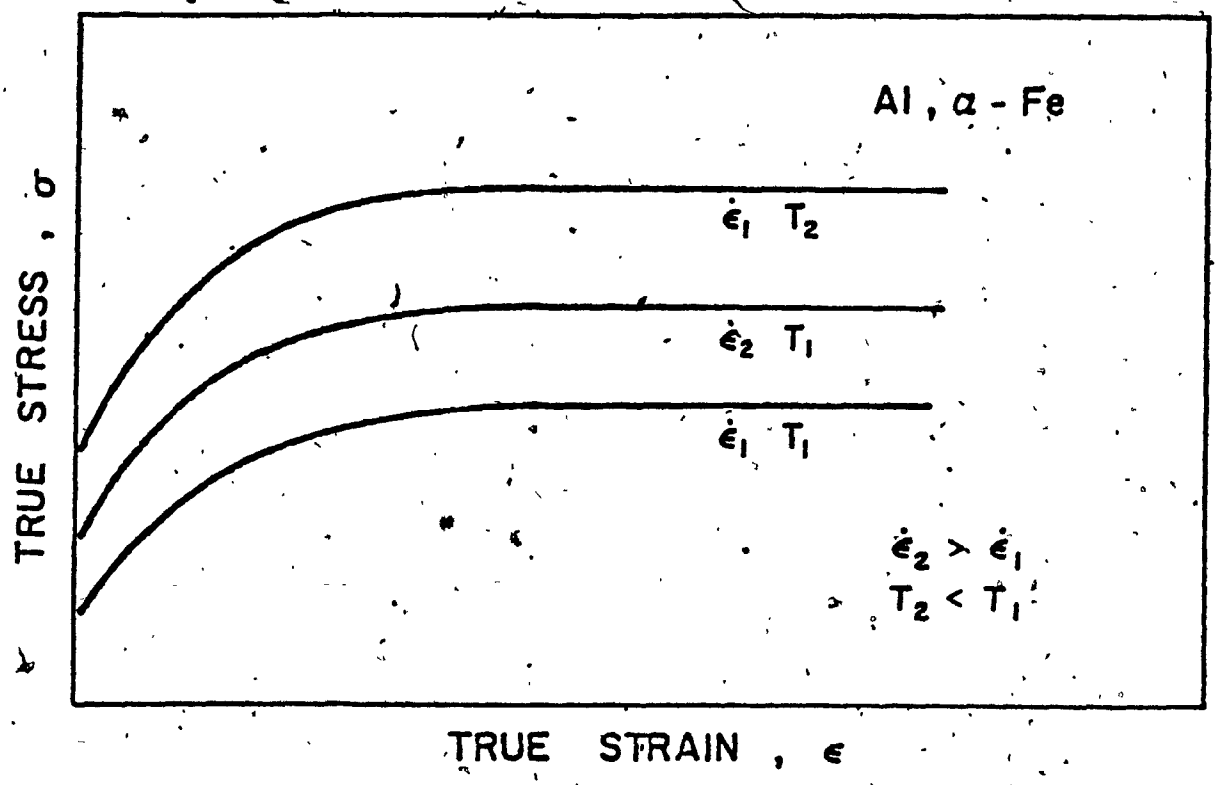

Fig. 2.1: Schematic Representation of the Flow Curve of Metals That Recover Dynamically.

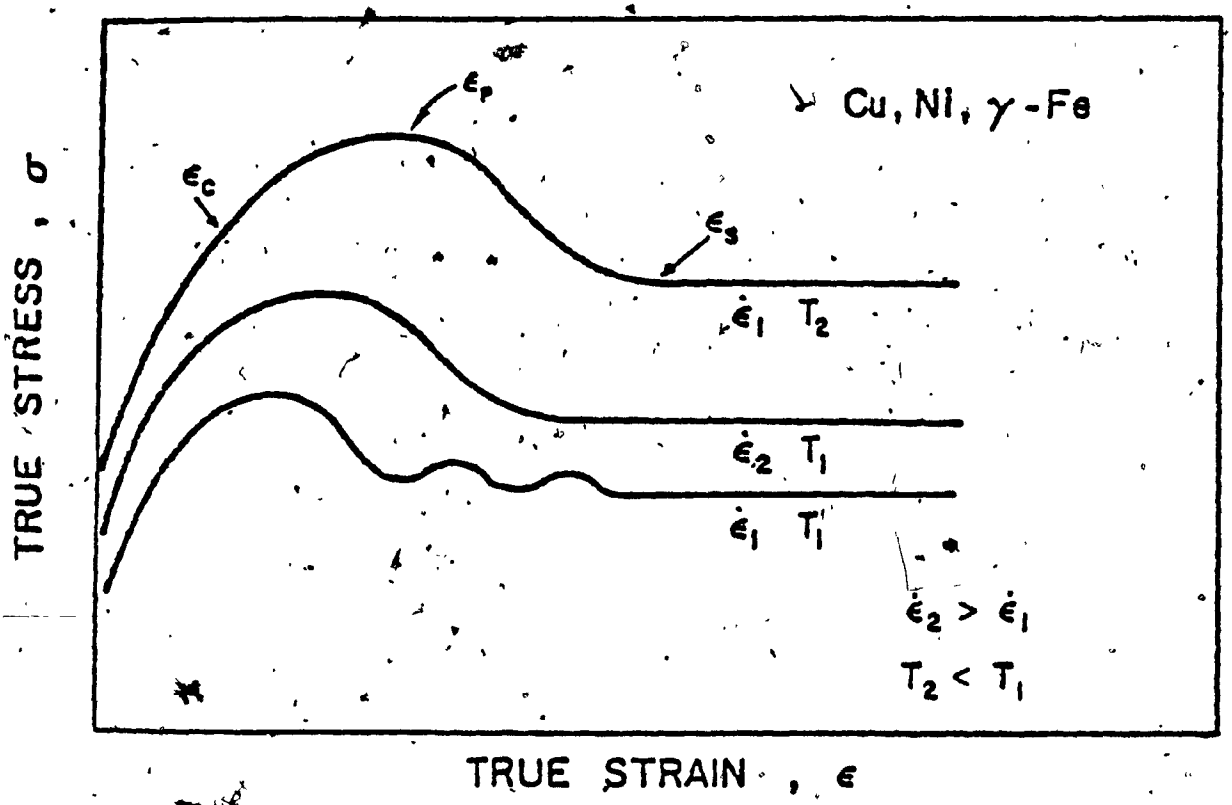

Fig. 2.2: Schematic Representation of the Flow Curves for Dynamic Recrystallization at High and Low Strain Rates.

At higher strain rates, the stress after the work softening remains constant (Fig. 2.2), indicating recrystallization is continuous as already described. At lower strain rates, recrystallization goes to completion and there is a stage of renewed hardening until recrystallization is again nucleated. This results in a cyclic flow stress after the peak (Fig. 2.2).

2.3 Static Restoration Process

Softening between passes or after completion of deformation is accomplished by static recovery, static recrystallization, or metadynamic recrystallization (Fig. 2.3). If the high temperature is maintained after recrystallization is completed, additional softening beyond the level of the starting material occurs due to the growth of the recrystallized grains.

a) Static Recovery

Static recovery involves dislocation annihilation and rearrangement in the sub-boundaries followed by growth of the subgrains (1,18,23). This process begins immediately when deformation stops and proceeds at a

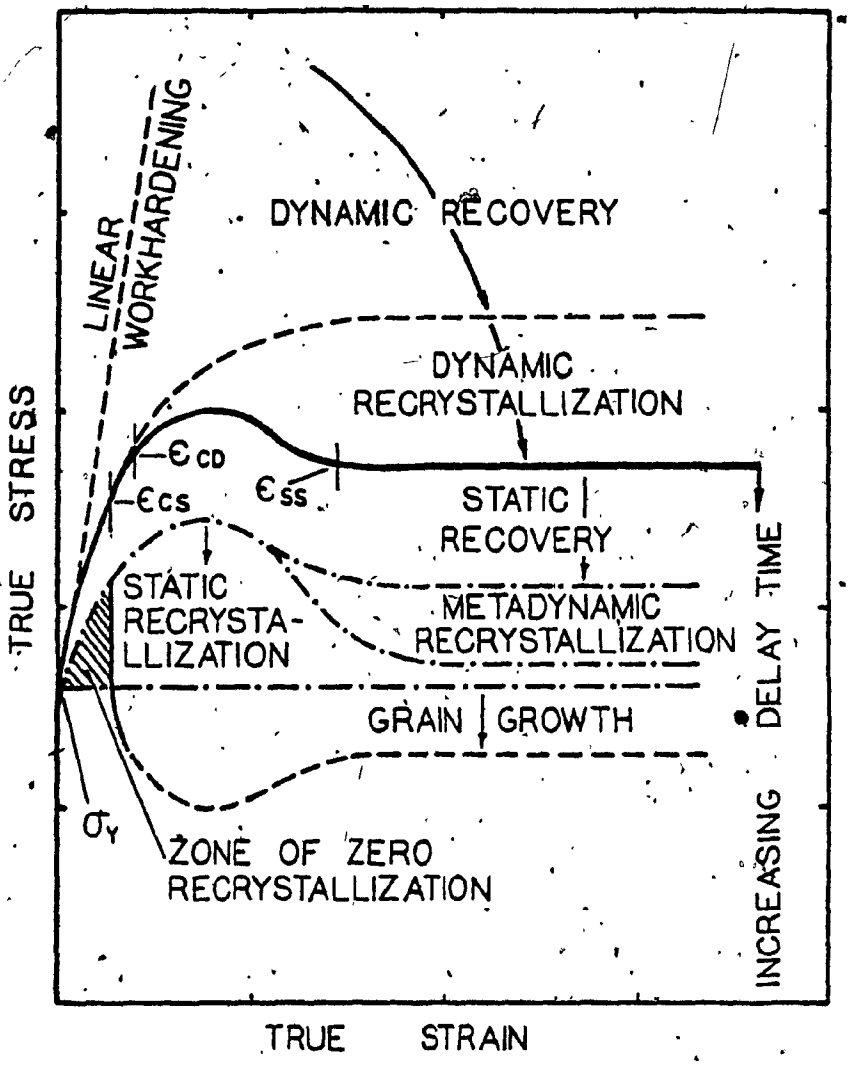

Fig. 2.3 Schematic Representation of Restoration Mechanisms.

decreasing rate as the dislocation density falls. An increase in temperature, pre-strain or strain rate increases the rate of static recovery. The addition of alloying elements usually decreases the rate of static recovery. Finally, it should be noted that full softening normally cannot be produced by recovery processes alone.

b) Static Recrystallization

Classical static recrystallization is preceded by an incubation period for nucleation and proceeds by migration of new boundaries until all the deformed grains are replaced. Raising the holding temperature has a dramatic effect in increasing the rate of static recrystallization (4,15,17,19). However, as the temperature of deformation is increased, the static recrystallization at a given temperature requires a higher critical strain, proceeds at slower rate and produces a larger grain size. The increased deformation temperature enhances the dynamic recovery thus lowering the dislocation density and hence the driving force for recrystallization. At a given temperature, the greater

the prestrain and the higher the strain rate, the larger is the driving force and therefore the faster the recrystallization (21). An increase in strain rate reduces the subgrain size and increases the sub-boundary density so there is a higher density of nucleation sites. An increase in strain during the work hardening region also increases the substructure density and nucleation rate but after steady state flow is achieved, strain does not have further influence on recrystallization rate (22). The increase in nucleation sites decreases the incubation times and therefore static recrystallization is accelerated.

The critical strain for static recrystallization is 0.15 to 0.20 which is far less than the critical strain for dynamic recrystallization (0.3 to 0.6) (24). The reason for this difference is that during dynamic recrystallization the grains are being deformed at the same time as they are being produced which tends to inhibit both nucleation and growth.

c) Metadynamic Recrystallization

The third type of softening occurring between passes is metadynamic recrystallization. Metadynamic recrystallization proceeds by the growth of recrystallization nuclei produced during deformation (7,19). Thus, no incubation period is involved, i.e., no time delay for recrystallization to start (7,20). This mechanism can only occur if the strain has exceeded the peak strain, i.e., the critical strain for dynamic recrystallization, otherwise no nuclei are present. Also, the nuclei of a metadynamically recrystallized metal contain a higher dislocation density than those in a statically recrystallized metal.

Both metadynamic recrystallization and static recovery require no incubation time so operate as soon as deformation ceases and account for a large fraction of the softening in short interruptions between passes. However, the softening obtained by recovery is far less than the softening obtained by static recrystallization. Metadynamic recrystallization can obtain 100% softening if continuous recrystallization in the steady state flow curve has been reached (19,20).

2.4 Effect of Niobium on Hot Working

The influence of niobium on the softening of steels during and after deformation depends upon whether the niobium exists in solid solution or as a carbonitride precipitate. In both forms it tends to reduce the size of the grains formed during dynamic, static or metadynamic recrystallization.

The increase in the flow curve up to the peak stress compared to the pure metal indicates that niobium makes dynamic recovery more difficult (1,25-27). From the results of Weiss, this retardation of recovery is due to the effects of both the niobium as a solute and precipitation of niobium carbides on the dislocation network. As a fine precipitate, however, NbC, can stabilize the substructure developed during dynamic recovery and hinder nucleation (28). The net result, in this case, is the retardation of dynamic recrystallization (strain to peak) and the prolongation of dynamic recovery as the sole restoration mechanism to a much higher strain.

During dynamic recrystallization, niobium, as a solute, has a drag effect on grain boundary migration while in the form of very fine carbonitrides, niobium pins grain boundary migration. Larger niobium carbides may act as sites for nucleation, thus reducing grain size (11). Insofar as niobium through these effects significantly reduces the grain size during dynamic (16), and also static or metadynamic (26,27,31) recrystallization, it results in a higher flow stress during deformation.

Static recovery is also retarded by addition of niobium to a steel (26,27). Again, it appears that this retardation is due to both solute effects and to precipitation of niobium carbides.

In the case of static recrystallization, a large increase in time for recrystallization has been noted when the niobium is in the solute form (26,27,32). This retardation of static recrystallization is largely due to the retardation of recovery. As a precipitate, niobium carbide can increase the time for fifty per cent recrystallization by two orders of magnitude (33,34,35).

2.5 Effect of Concurrent Precipitation on Recrystallization

Both precipitation and recrystallization involve dislocations. The precipitation reactions uses dislocations as nucleation sites while recrystallization requires a dislocation substructure for nucleation and as a driving force. The relative effect of dislocations on each reaction is among other things, temperature and prestrain dependent (25-27,30).

Investigators have found the precipitation of niobium carbides begins earlier and proceeds fastest at 900° C, (Fig. 2.4) (26,27). This optimum temperature is a result of an increase in driving force as the temperature decreases - more niobium carbides are forced out of solution and a decrease in atomic mobility as the temperature lowers. Since precipitates hinder recrystallization, rapid precipitation at 900° C results in an abnormally slow recrystallization reaction at this temperature. The resultant curve for recrystallization has a reverse knee at 900° C (Fig. 2.5) (26,27).

Superposition of precipitation and recrystallization curves (Fig. 2.6) indicates that at 900° C recrystallization does not start until nearly all the niobium has precipitated. These curves also show that whenever precipitation starts before recrystallization, static recrystallization is retarded.

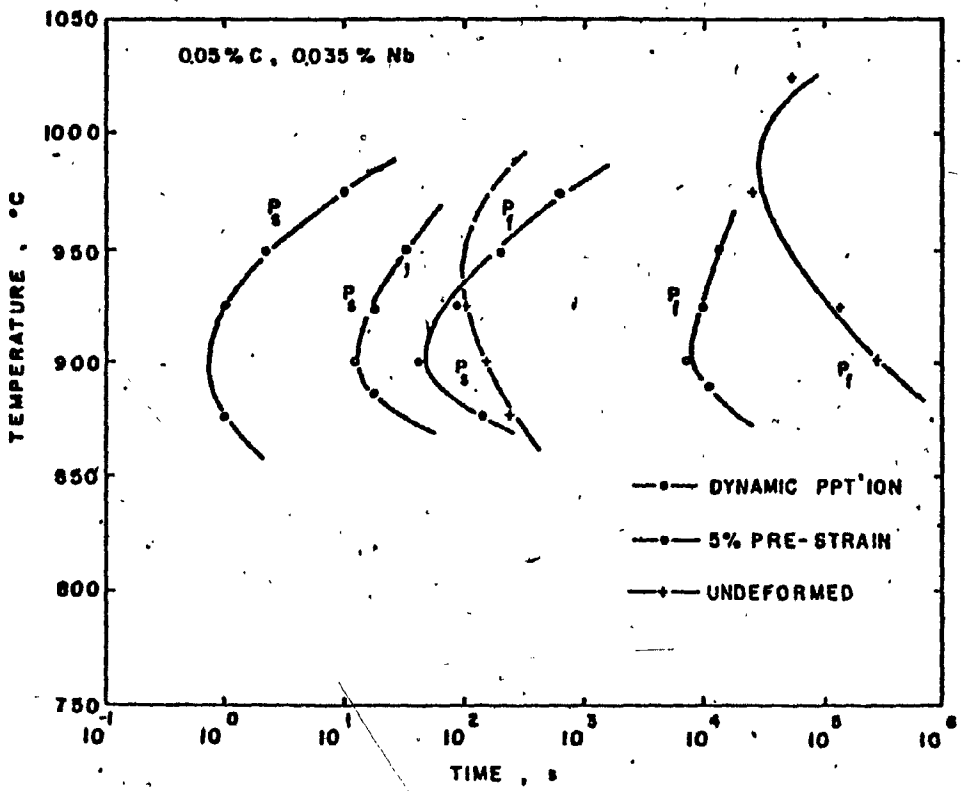

Fig. 2.4 Precipitation Start and Finish Times in Undeformed, Predeformed and Deforming Austenite, (Weiss (27)).

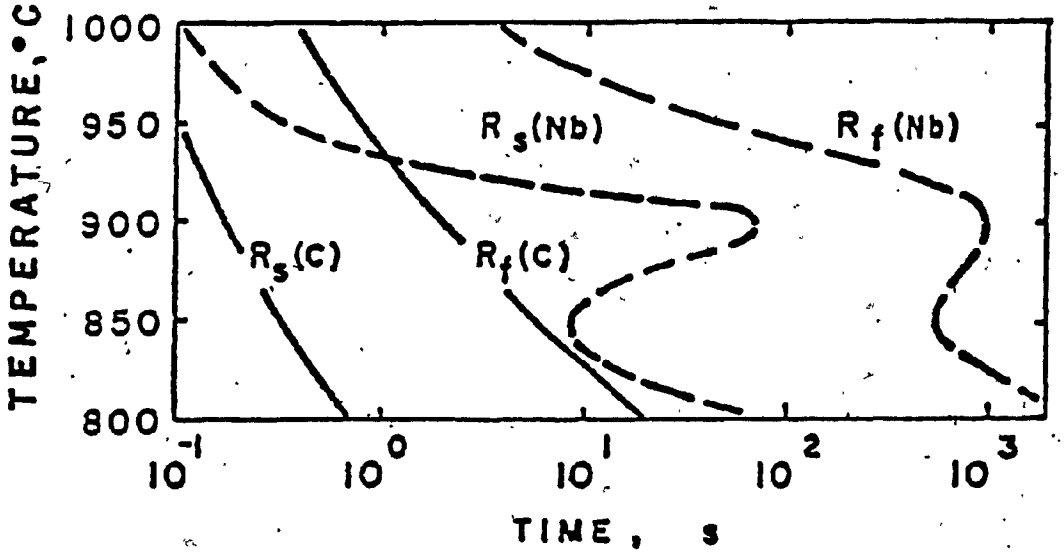

Fig. 2.5 Recrystallization - Temperature - Time Diagram for a 0.17%C - 0.04%Nb Steel (LeBon et al (29)).

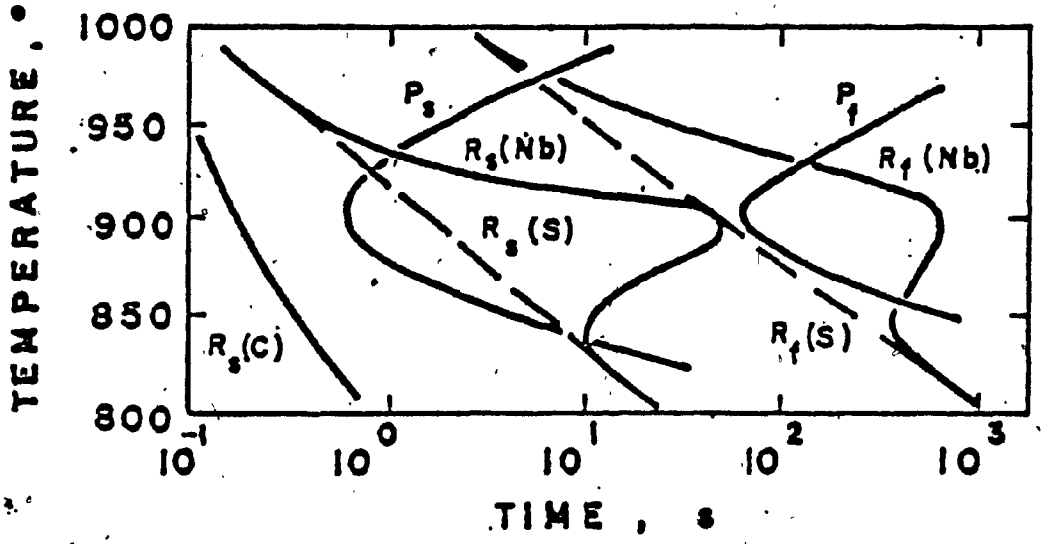

Fig.2.6 The Interaction between Precipitation and Recrystallization.

CHAPTER 3

Experimental Procedure

3.1 Torsion Testing

In the present work, the torsion test was used to determine the hot working properties of HSLA steels. In particular, a hot mill with coilers was simulated. Although the torsion test produces a variation of strain and strain rate (from zero on the axis of rotation to a maximum in the outer fibers), it permits deformation at high constant strain rates. Since neither necking nor barrelling occurs, the true strain and strain rate are equal to the engineering strain and strain rate (2).

For these trials, the angle of twist and the twist rate were controlled by a closed loop "MTS" system (Fig. 3.1). The data, in the form of torque versus angular displacement, was recorded on a Hewlett-Packard x - y recorder. In the continuous trials at $10s^{-1}$, a computer was used to control the test, to gather the data and to plot torque versus angular displacement graphs.

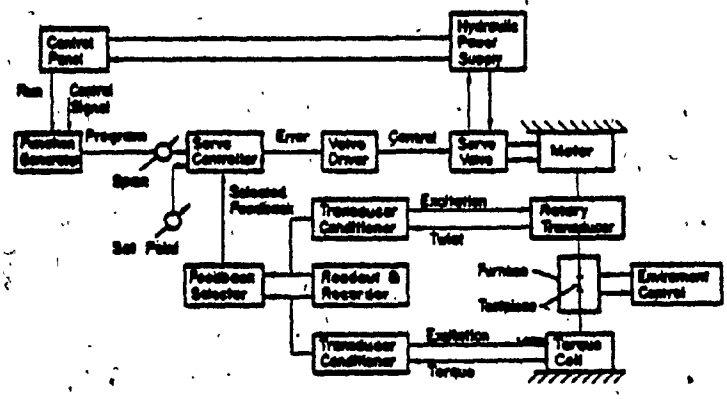

Fig. 3.1 The Control System

The following formula was used to convert torque to shear stress (36 - 38):

$$\tau = M_T (3 + m + n^1) / 2\pi r^3$$

where M_T - torsional moment

m - strain rate sensitivity

n^1 - strain hardening exponent

r - radius of the gauge section

Since all experiments were conducted above 0.5 Tm where the strain hardening exponent, n^1, is small, m is the dominant parameter (37 - 39). For all calculations, the value of m was 0.15 (based on Rossard's analysis) (36, 40) and n^1 was zero since correlation was made for the peak or for the steady state region.

The torsional strain at the surface of the specimen was calculated using the following formula (41):

$$\gamma = \frac{2\pi rN}{Lo}$$

where N - the number of turns

Lo - the original gauge length

To convert shear stresses and strains to effective stresses and strains, the von Mises criterion for plastic yielding was used (42):

$$\text{Equivalent stress, } \bar{\sigma} = \sqrt{3}\,\tau$$

$$\text{Equivalent strain, } \bar{e} = \gamma/\sqrt{3}$$

These conversions enable the results obtained by the torsion test to be compared to data gathered by other investigators using tension and compression tests.

3.2 Torsion Testing Equipment

As mentioned previously, these tests were conducted on a torsion tester controlled by a closed loop "MTS" system. The torsion machine is capable of applying a maximum torque of 110 Nm at velocities up to 15 revolutions per second to a maximum of 100 revolutions.

The closed loop "MTS" system controlled a hydraulic motor which imparted the required angular displacement to a superalloy loading bar which in turn transmitted this rotation to the specimen. The other end of the specimen was held by a superalloy reaction bar fixed to a torque

cell. The rotary displacement was measured by a dual gang potentiometer. A detailed description of the torsion machine has been given by Fulop et al (43).

The specimen was heated by a radiant furnace which can attain 1100^{o} C. The furnace was purged with argon gas during the experiments to reduce the amount of oxidation occurring during the tests. Also, a carbon black strip was applied to the center of the furnace so that the temperature did not vary more than $\pm$ 1^{o} C along the gauge length of the specimen. The test temperature was controlled by means of a thermocouple extending into the shoulder of the test specimen. This thermocouple had been previously calibrated against a thermocouple embedded in the gauge section.

3.3 Test Materials

The torsion test specimens used in these studies were machined from 0.625" thick niobium bearing steel (HSLA) plate supplied by SIDBEC-DOSCO Steels Ltd. The chemical composition of the steel is listed in table 3.1.

Table 3-1 Chemical Composition in wt% of Steel Tested

Element	%wt
C	0.12
Mn	0.94
S	0.016
P	0.0
Si	0.007
Cu	0.09
Ni	0.04
Cr	0.04
Mo	0.007
Sn	0.01
Ti	0.000
Al	0.005
V	0.002
Nb	0.05
N_2 (ppm)	45

The torsion test pieces were removed from the plate in such a manner that their axis coincided with the rolling direction. The test specimen was threaded on one end while the other end was rectangular in shape. The rectangular end provided easy positioning and removal of the specimen and permitted free longitudinal motion during heating and deformation (Fig. 3.2).

To insure the niobium carbide was dissolved, the specimens were heated, prior to testing, to 1250° C for 30 minutes and then quenched.

3.4 Test Procedures

The specimens were mounted into the grips with Target Sure Turn* high temperature anti-sieze compound. The temperature was then raised within 5 minutes to the test temperature. In the case of tests conducted at 800 and 850° C, the specimen was preheated to 900° C for 5 minutes and then cooled to the test temperature. This was done to insure that the steel had transformed to austenite.

* Registered trademark of Releasall Ltd., Montreal

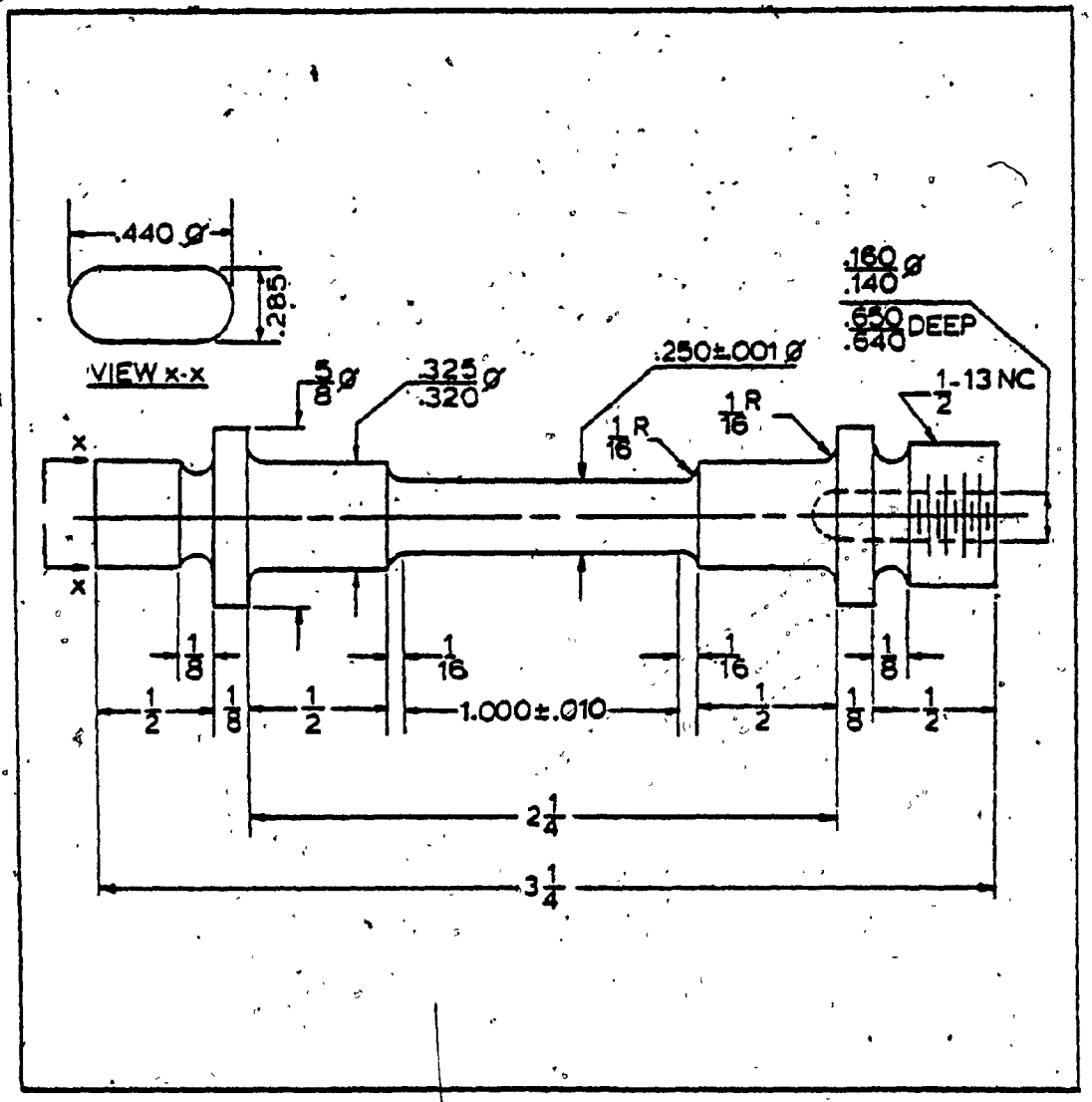

Fig. 3.2: Test Piece Design(in inches).

The first set of tests were done without interruption to fracture or to the 50 turn capacity of the machine. These tests were conducted at 800, 850, 900, 950 and 1000° C at strain rates of 0.1 and 1.0s^{-1}. Tests were also conducted at 900, 950 and 1000° C at a strain rate of 10s^{-1}.

The second set of tests simulated the end of a slab passing through a reversing mill. This was accomplished by interrupting at a strain of 0.3 and holding for interruptions alternating in duration from 150 to 10 seconds. The alternating interruptions simulate the time it takes the end of the slab to pass once again through the rolls. The short intervals simulate the case where the end of the slab leaves the rolls last and immediately re-enters them upon reversing. The 150 second interval simulates the case where the end of the slab leaves the rolls first, and upon reversing, enters the rolls last. During this time the slab is coiled into a furnace to maintain its temperature. These tests were conducted at 800, 850, 900, 950 and 1000° C at strain rates of 0.1s^{-1}.

Other trials were conducted at a strain rate of $1.0s^{-1}$ with interruptions at pass strains of 2.5 for 10 seconds. These tests were conducted at 900, 950 and 1000° C. One test was also conducted at 950° and at a strain rate of $10s^{-1}$ with interruptions at strains of 4.0 for 20 seconds.

The fractional softening which occurred during the interruptions was calculated by taking the ratio of the difference in stress at the instant of unloading and at the beginning of reloading to the increases in stress due to strain hardening during the first cycle of strain. Figure 3.3 shows the method of data analysis.

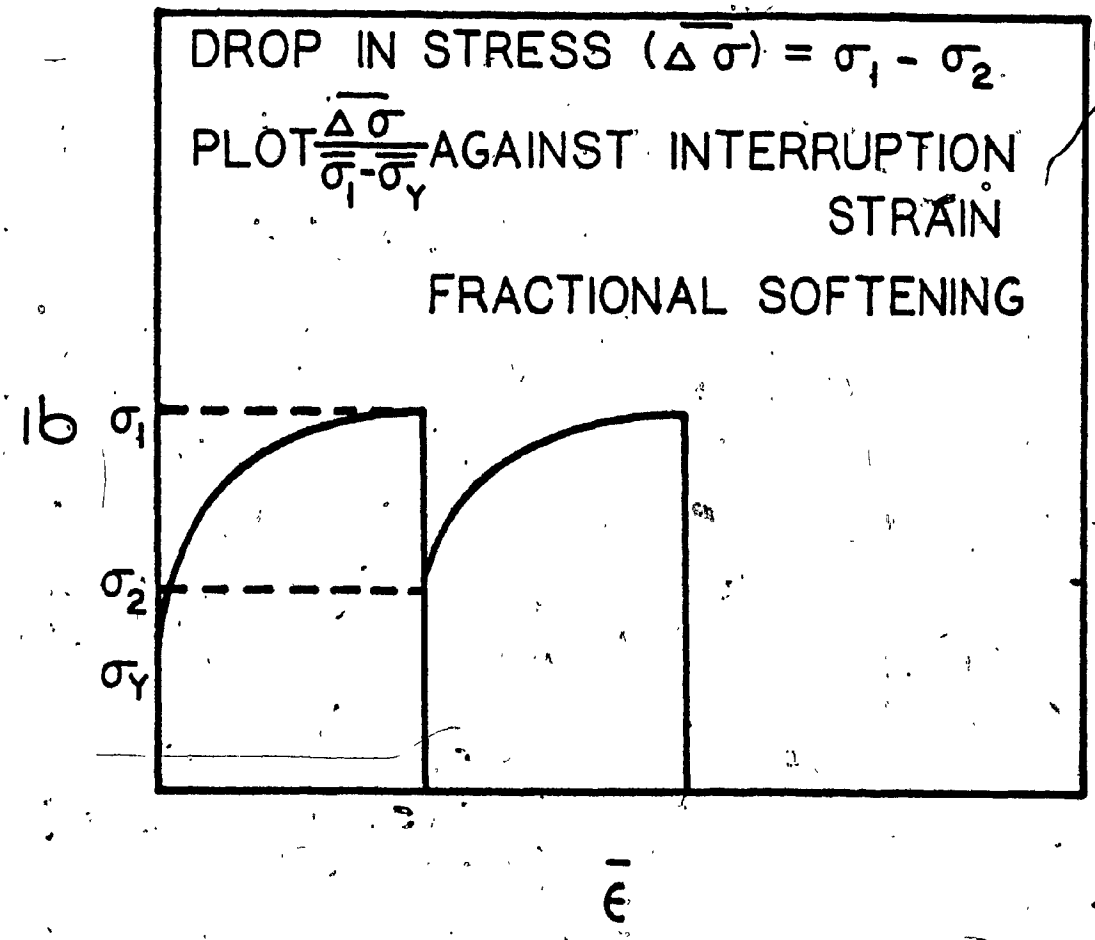

Fig. 3.3 Method of Data Analysis.

CHAPTER 4

Experimental Results

As explained in the previous chapter, the recorded torque and twist data were converted to equivalent stress ($\bar{\sigma}$) and strain ($\bar{e}$). These values were then plotted and will be presented in this chapter.

4.1 Continuous Deformation

The equivalent stress-strain plots obtained during continuous deformation at various test conditions are shown in figure 4.1. The curves exhibit a peak stress followed by a steady state region. A plot of strain to peak stress, $\bar{e}p$, versus temperature (Fig. 4.2) indicates that $\bar{e}p$ decreases with temperature and increases with strain rate.

The results of these tests were also compared to previous data. In particular, plots of log $\dot{e}$ versus log $\bar{\sigma}$ (Fig. 4.3a) and log $\bar{\sigma}$ versus $^{1}/_{T}$ (Fig. 4.3b) compares the results obtained at $10s^{-1}$ to those obtained by Sankar (36) at strain rates of 0.1 and $1.0s^{-1}$. The slopes of these lines indicate that the following relationship applies:

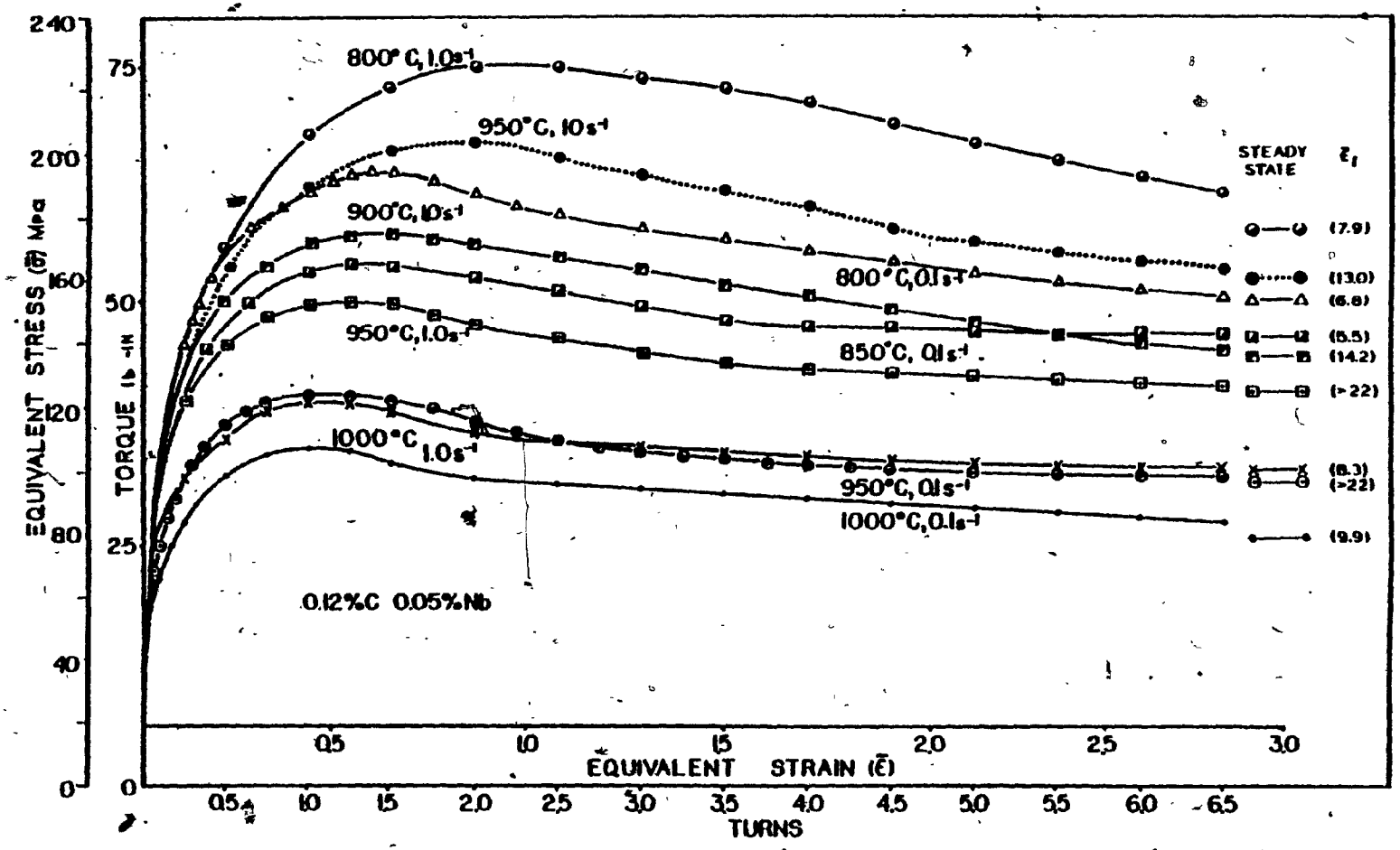

Fig. 4.1 Continuous Flow Curves for a 0.12% C. 0.05% Nb Steel at Various Temperatures and Strain Rates.

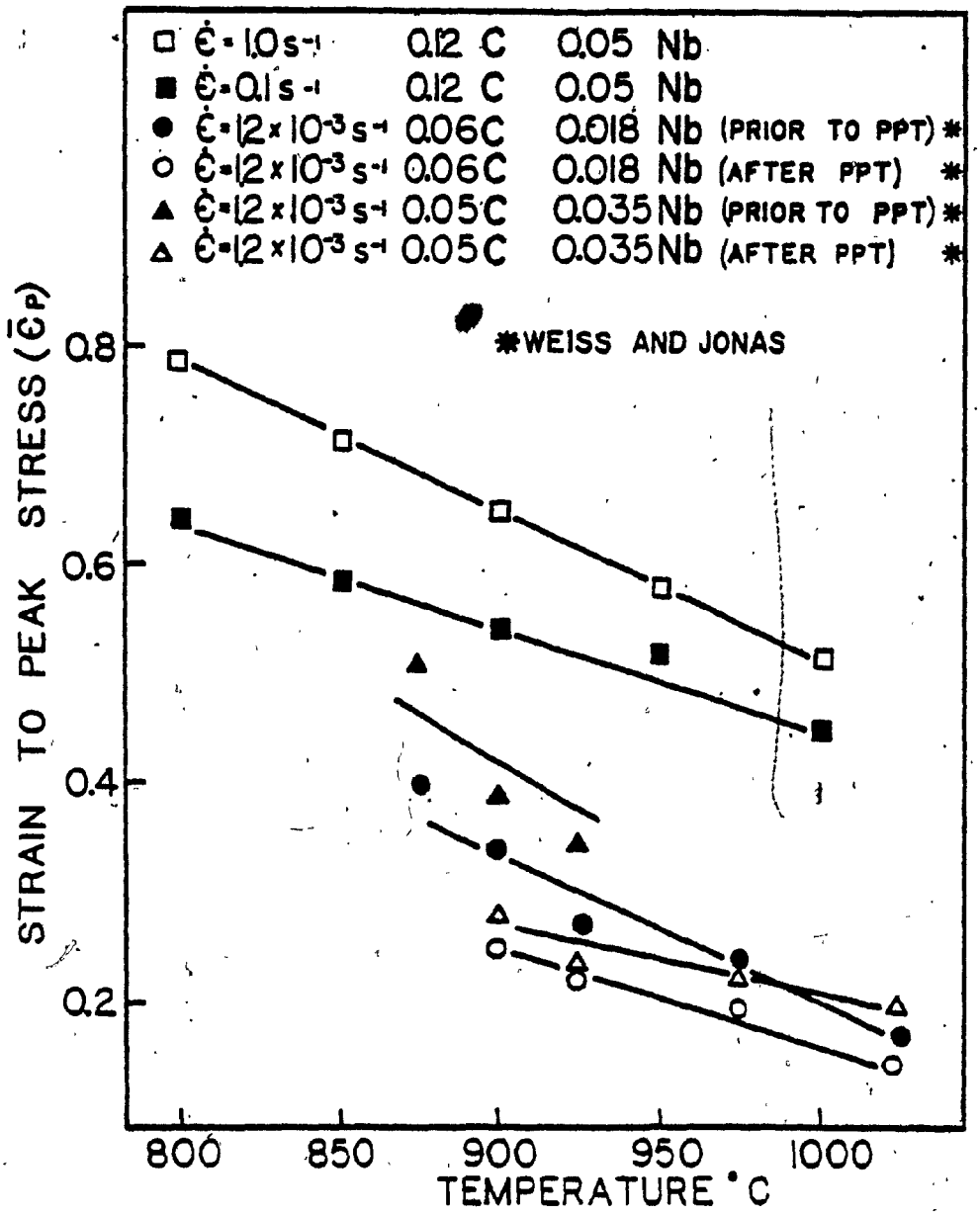

Fig. 4.2 Dependence of Strain to Peak Stress on Temperature, Strain Rate and Composition.

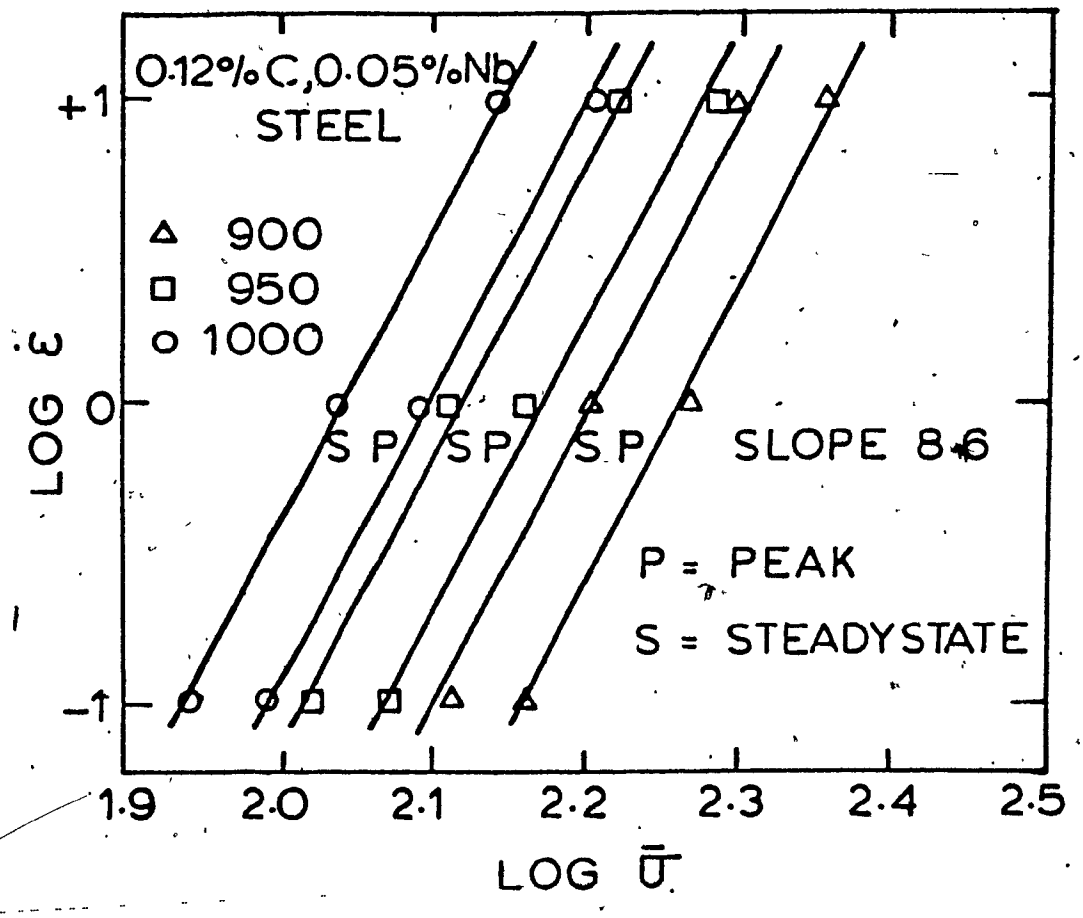

Fig. 4.3a Stress Dependence of the Strain Rate of 0.12% C, 0.05% Nb Steel at Various Temperatures. Revision of Plot by Sankar (36).

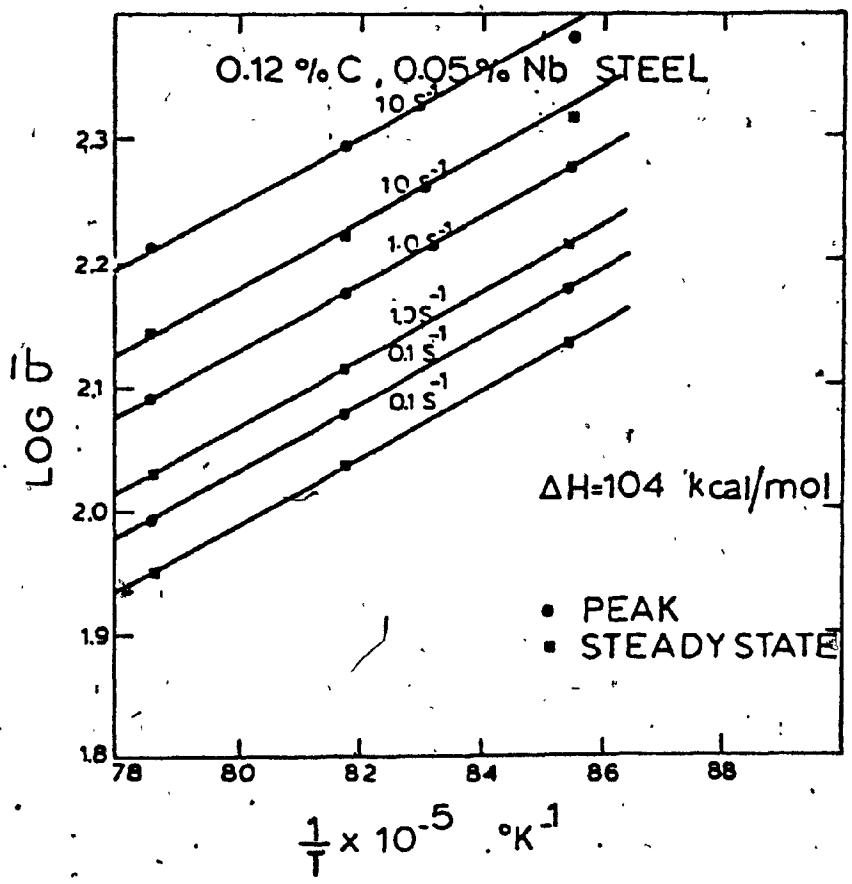

Fig. 4.3b Temperature Dependence of the Peak and Steady State Stress for a 0.12% C, 0.05% Nb Steel at Various Strain Rates. Revision of a Plot by Sankar (36).

$$\dot{e} = A\sigma^n \exp(-\Delta H/RT)$$

where $\dot{e}$ - strain rate

A - constant

σ - flow stress

n - stress exponent

ΔH - activation energy

R - gas constant

T - temperature in degrees absolute

4.2 Interrupted Tests

Test curves for interrupted deformations at a strain rate of $0.1s^{-1}$ are presented in figures 4.4 and 4.5. The interruptions at pass strains of 0.3 have alternating durations of 150 and 10 seconds. The broken lines on these graphs are the corresponding continuous deformation curves. At the higher strain rate of $1.0s^{-1}$, the interruptions were at strains of 2.5 for 10 seconds. These curves for 900, 950 and 1000° C with the corresponding continuous curves superimposed are presented in figure 4.6. Figure 4.7 gives the stress-strain curve for the test conducted at 950° C and a strain rate of $10s^{-1}$ with interruptions at a strain of 4.0 for 20 seconds each.

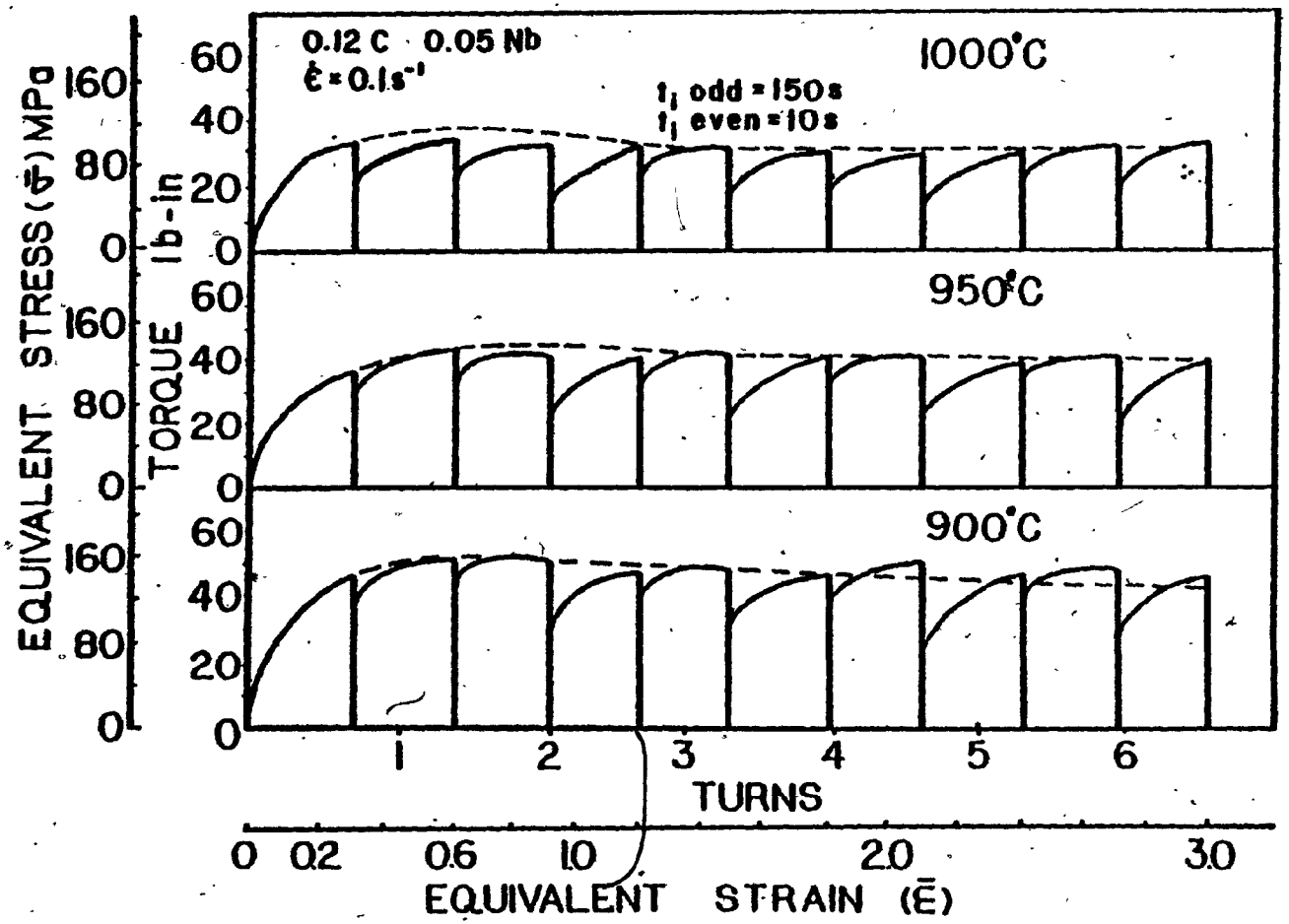

Fig. 4.4 Interrupted Flow Curves for a 0.12% C, 0.05% Nb Steel at $0.1 s^{-1}$ and at 900, 950 and 1000° C with Pass Strains of 0.3 and Alternating Interruption Times of 150 and 10 seconds.

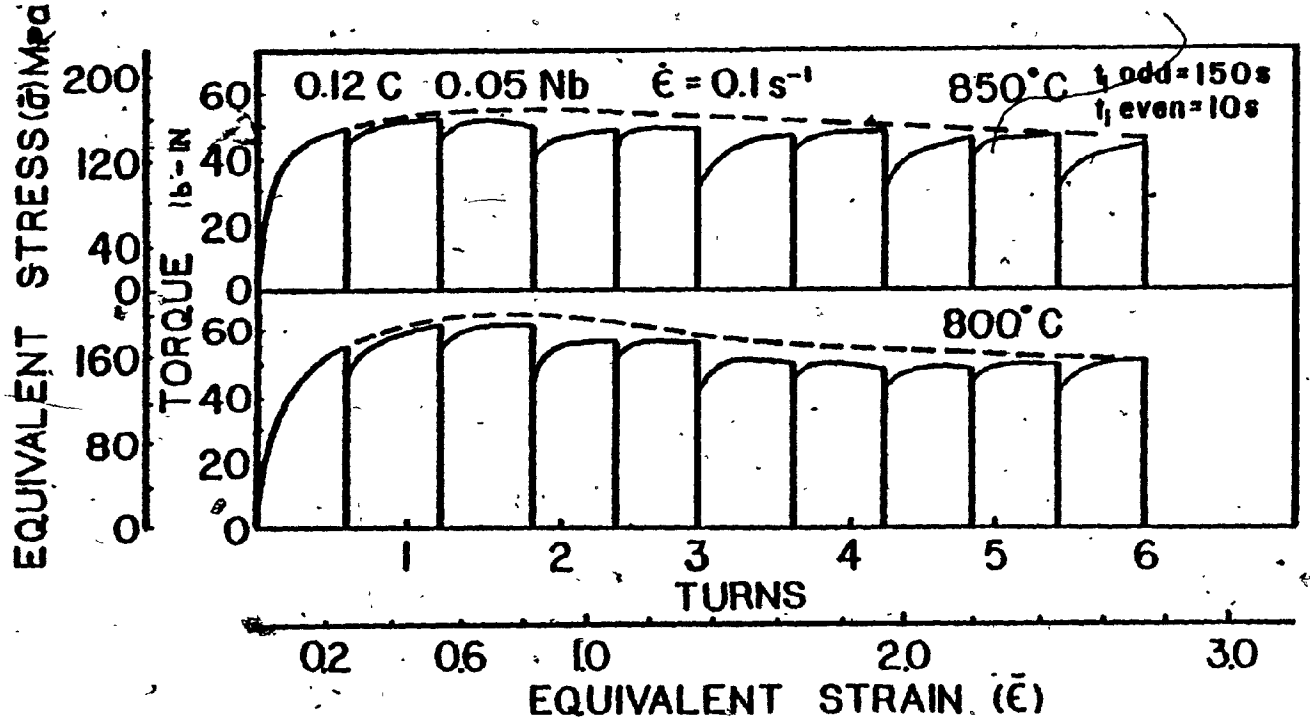

Fig. 4.5 Interrupted Flow Curves for a 0.12% C, 0.05% Nb Steel at $0.1s^{-1}$ and at 800 and 850° C with Pass Strains of 0.3 and Alternating Interruption Times of 150 and 10 Seconds.

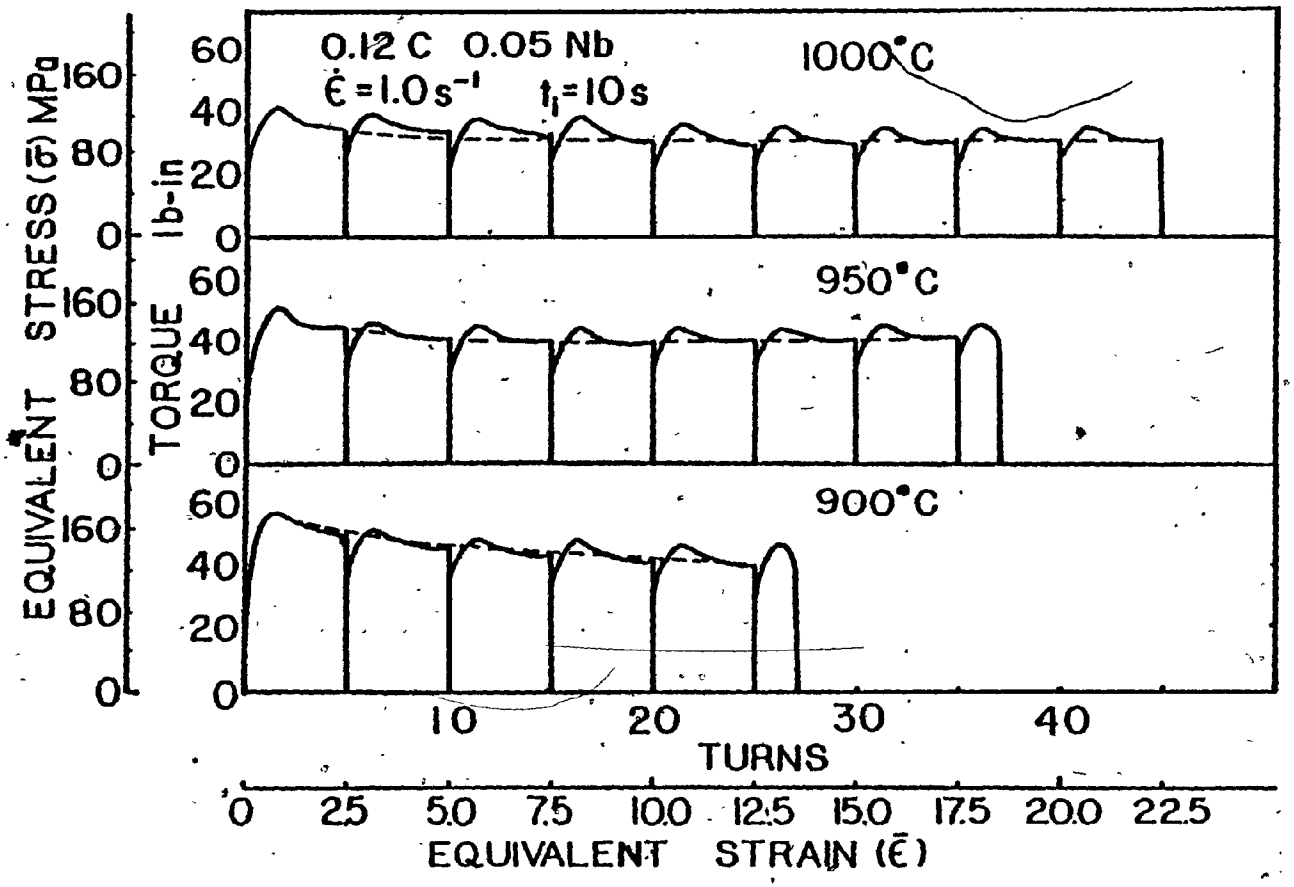

Fig. 4.6 Interrupted Flow Curves for 0.12% C, 0.05% Nb Steel at 1.0s^{-1} and at 900, 950 and 1000° C for Pass Strains of 2.5 with 10 Second Interruptions.

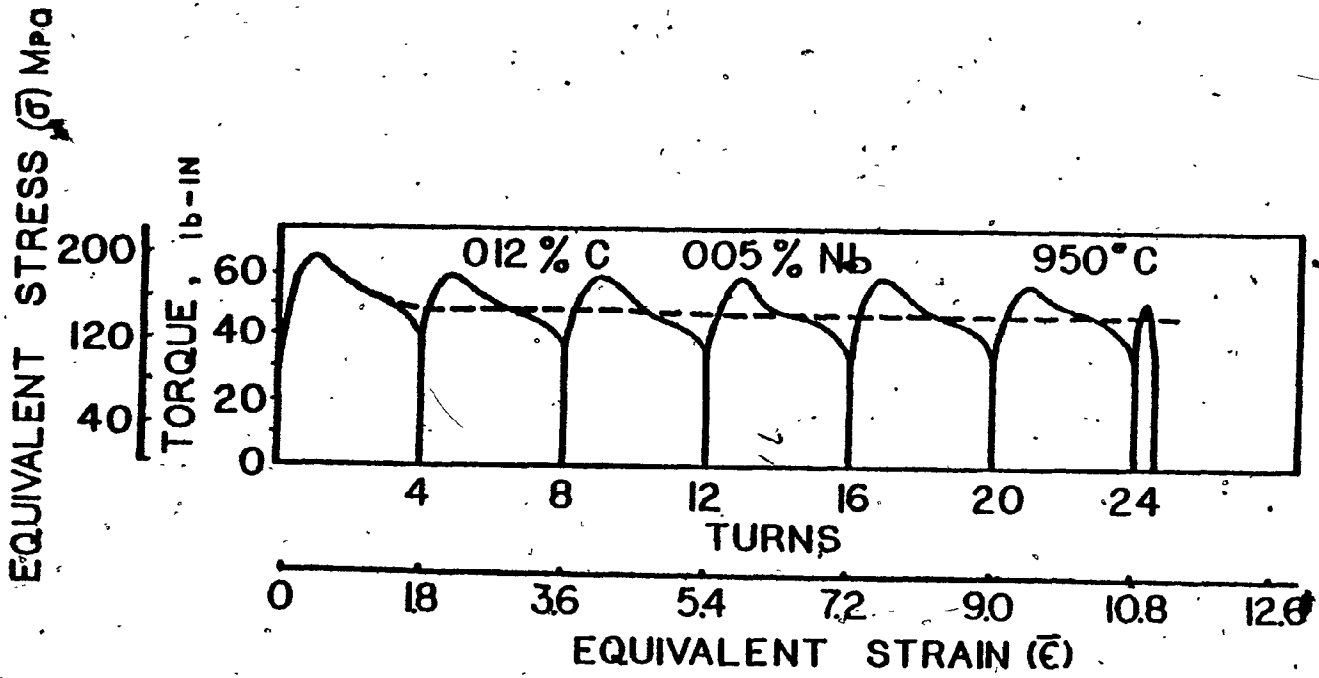

Fig. 4.7 Interrupted Flow Curves for 0.12% C, 0.05% Nb Steel at $10s^{-1}$ and at 950° C for Pass Strains of 4.0 with 20 Second Interruptions.

To clearly show the static restoration between passes, the fractional softening during each interval is plotted against the accumulated strain. Figure 4.8 indicates the fractional softening which occurred during the 150 and 10 second interruptions at strain rates of $0.1s^{-1}$. The fractional softenings during these tests are compared in figure 4.9 to those obtained under somewhat different conditions by Sankar (36). The average fractional softening during the 10 and 150 second interruptions are plotted against $^{1}/_{T}$ in figure 4.10. The fractional softening at the higher strain rates (1.0 and $10s^{-1}$) are shown in figure 4.11.

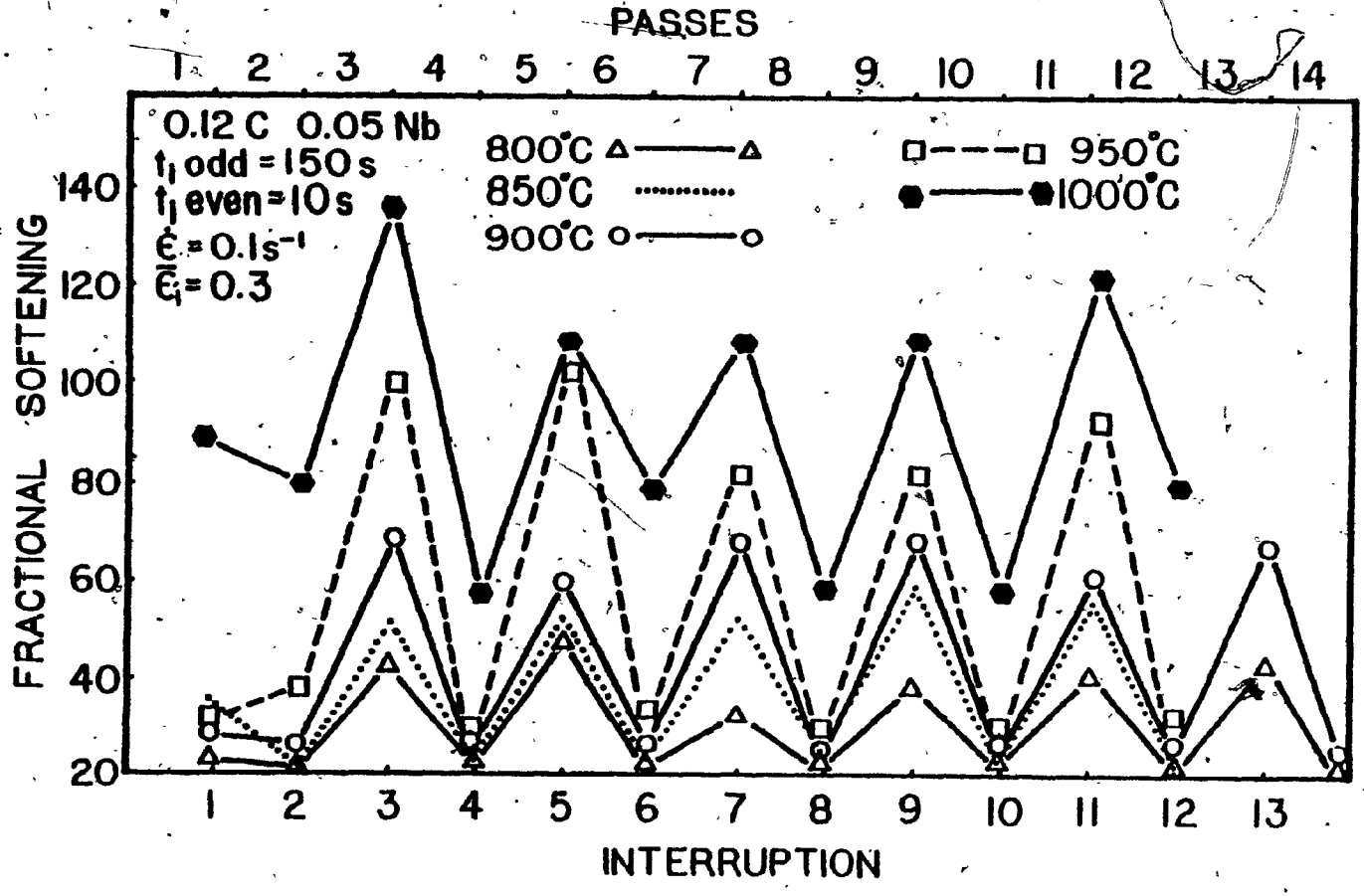

Fig. 4.8 Variation of Fractional Softening with Temperature, Interruption Time and Accumulated Strain for a 0.12% C, 0.05% Nb Steel Strained at 0.1s^{-1} with Alternating Pauses of 150 and 10 Seconds at Strains of 0.3.

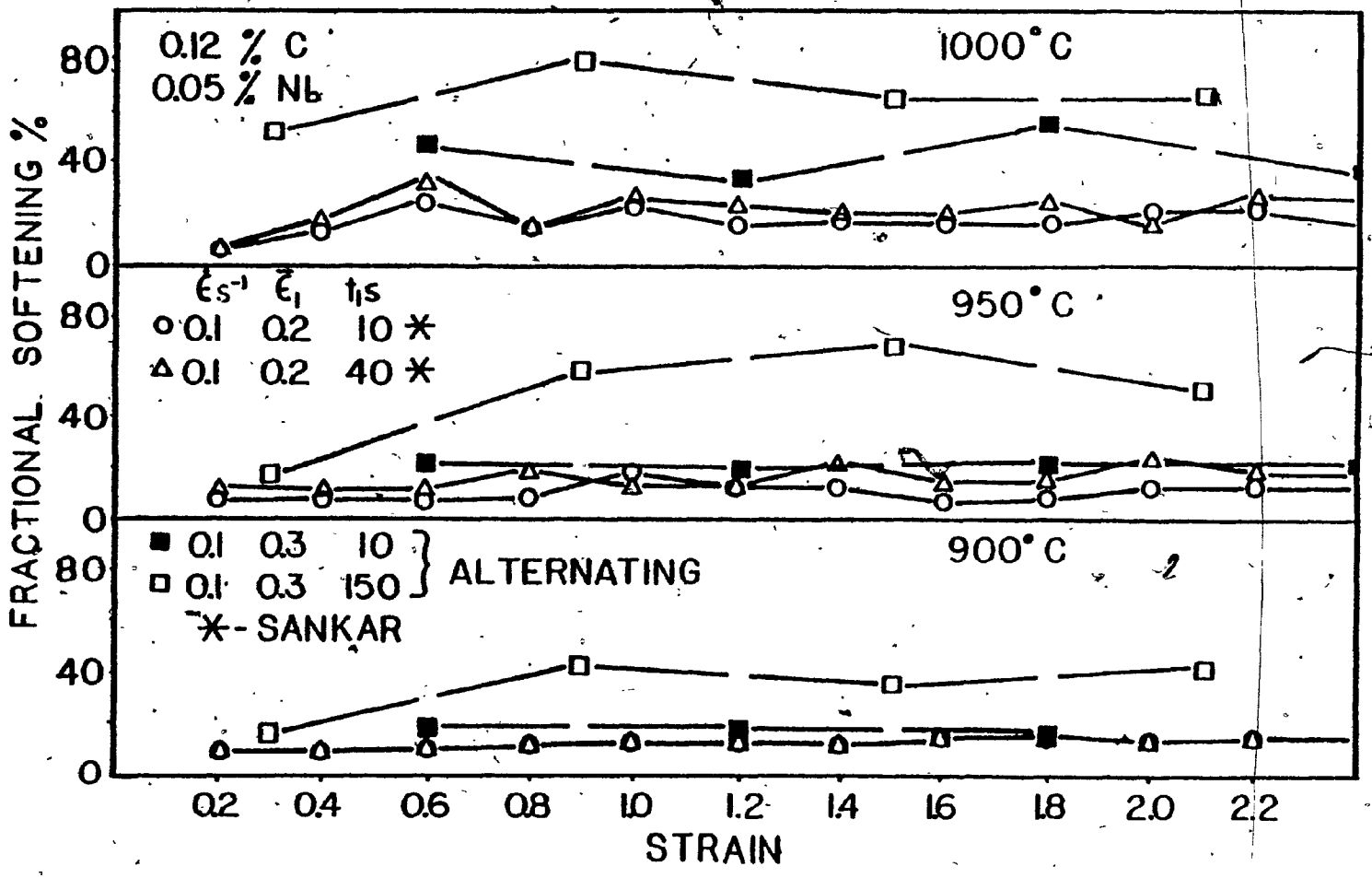

Fig. 4.9 Comparison of Fractional Softening Obtained in Present Study to Sankar (36).

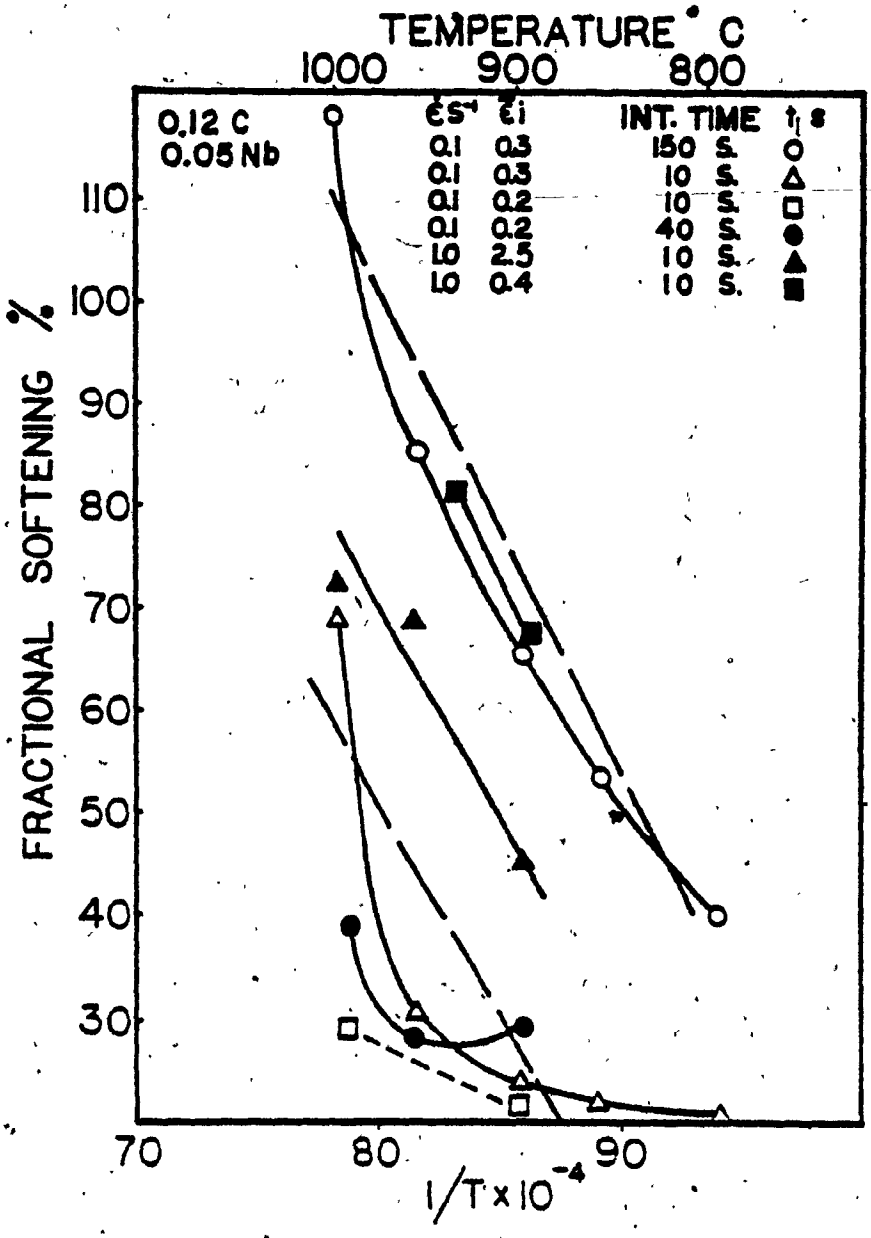

Fig. 4.10 Relation of Fractional Softening to Temperature for 10 and 150 Second Pauses.

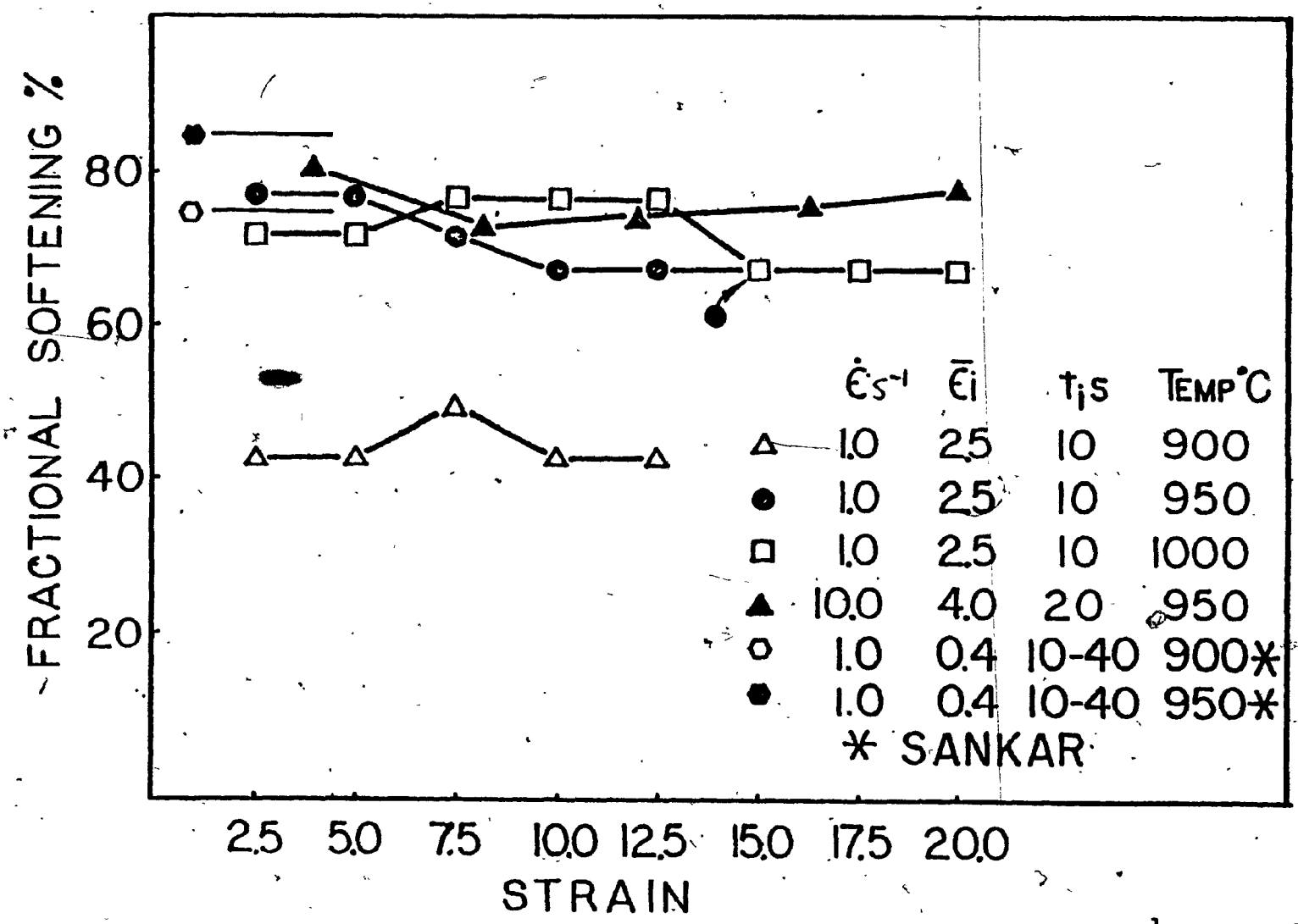

Fig. 4.11 Fractional Softening for 0.12% C, 0.05% Nb Steel Strained at $1.0s^{-1}$ and $10s^{-1}$.

CHAPTER 5

Discussion

5.1 Continuous Deformation

The stress-strain graphs (Fig. 4.1) for all conditions tested consist of a peak stress followed by work softening to a steady state region. This shape indicates that dynamic recrystallization is occurring (17,44). At constant strain rate, a rise in temperature lowers the peak and steady state stress indicating that recrystallization is more rapid and larger grains are produced. The lower flow stress can also be attributed to the less dense substructure in the deformed region due to the higher degree of dynamic recovery.

At constant temperature, an increase in strain rate raises the peak and steady state stresses. The higher strain rate produces a finer grain and sub-grain structure as a result of a decrease in the amount of dynamic recovery per unit strain. In these tests it was noted that increasing the strain rate by one order of magnitude is approximately equivalent to lowering the temperature 50° C; for example, the curve for 950° C and $0.1s^{-1}$ is almost identical to that for 1000° C and $1.0s^{-1}$.

The amount of decrease in flow stress from 850° to 900 ° C, is much less than the decrease from 900 to 950° C (Fig. 4.1). This abnormally high flow stress at 900° C is probably due to the retardation of dynamic recrystallization caused by the concurrent precipitation of niobium (26,27,29) which proceeds more rapidly at this temperature than at either 850° or 950° C.

In addition, the strain required to reach the peak stress, $\bar{\epsilon}p$, is raised by an increase in strain rate at a constant temperature or a decrease in temperature at a constant strain rate (Fig. 4.2). The increase in $\bar{\epsilon}p$ with decreasing temperature is attributable to a decreased rate of nucleation even though the stored energy is greater. In the case of increase of strain rate at constant temperature, the critical strain for recrystallization is greater although the stored energy at any strain is higher, thereby indicating that concurrent deformation hinders the recrystallization.

The new data at $10s^{-1}$ caused a revision of the $\log \bar{\sigma} - \log \dot{\epsilon}$ (Fig. 4.3a) and the $\log \bar{\sigma} - {}^{1}/_{T}$ (Fig. 4.3b) plots made by Sankar (36) with the result that the value of

n was found to be 8.6 rather than 8.3 and ΔH is approximately 104 Kcal/mole rather than 101.2 Kcal/mole. These results, however, cannot be adequately compared to the work of other people due to the lack of published data in this area.

5.2 Interrupted Deformation

Softening during the intervals between passes can be attributed to one or several of the following mechanisms: static recovery, static recrystallization, metadynamic recrystallization, and grain growth following recrystallization. At strains below the critical value for static recrystallization or during short interruptions, softening occurs only as a result of static recovery. An example of this is found in the results of Sankar (36) for interrupted tests at 900° C and $0.1s^{-1}$ in which the fractional softening is approximately 25% (Fig. 5.1a). At higher strain rates ($1s^{-1}$) or during long interruptions (40s) recrystallization produces large drops in the flow curves and softening of 75 - 100% (Fig. 5.1b).

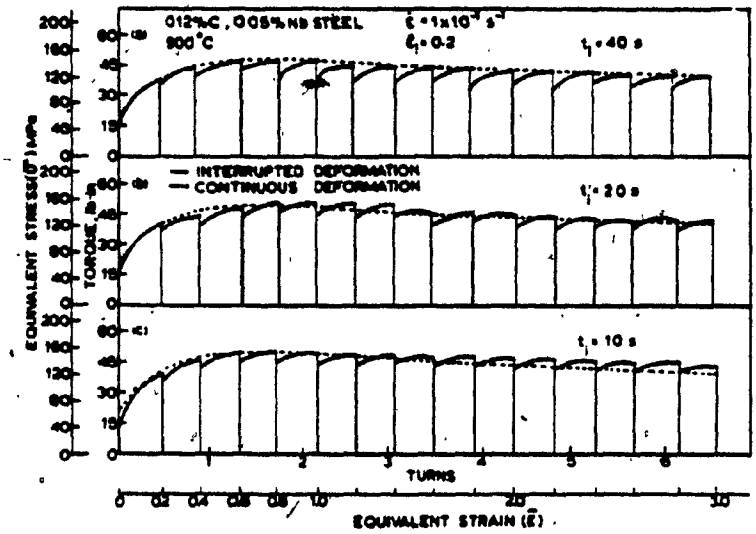

Fig. 5.1a Interrupted Flow Curves for Nb Steel Strained at 900° C and $0.1s^{-1}$ with Pass Strains of 0.2.

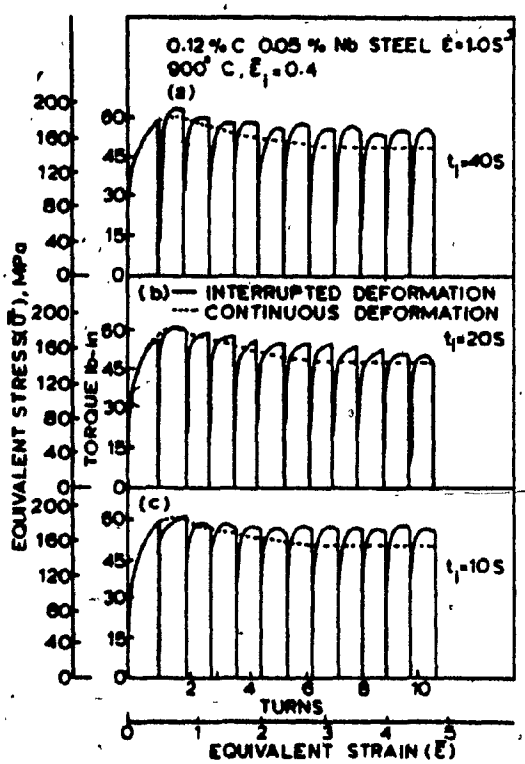

Fig. 5.1b Interrupted Flow Curves for Nb Steel Strained at 900° C and $1.0s^{-1}$ with Pass Strains of 0.2.

The effects of different hold times and temperatures can be seen in the stress-strain graphs at a strain rate of $0.1s^{-1}$ with interruptions occurring at pass strain of 0.3 (Figs. 4.4 and 4.5). The odd numbered interruptions are 150 seconds in duration while the even ones are only 10 seconds long. The first interruption of 150 seconds at all temperatures except 1000° C has a fractional softening between 20 and 35% (Fig. 4.8), thereby indicating that static recovery is the only mechanism operating. In addition, upon reloading the stress-strain curve returns to match the continuous one after only a small strain. The large amount of softening at 1000° C indicates recrystallization is occurring during the first interruption.

During the short interruptions of 10 seconds, the amount of softening is also small, with the exception of 1000° C, indicating that again static recovery is the only mechanism operating. Partial recrystallization is taking place in the 1000° C test and possibly to a small extent in the 950° C test. However, varying the temperature between 800 and 900° C seems to have little effect on the amount of softening at this short time.

In the long interruptions, starting with the third interruption, softening is large enough to indicate that recrystallization is occurring. Raising the temperature considerably increases the amount of softening during these 150 second holds until almost complete recrystallization (100% softening) occurs at 950° C. At 1000° C, more than 100% softening occurs indicating that recrystallization is followed by a grain growth resulting in a final grain size which exceeds the original.

The occurrence of either recovery or recrystallization is also noticeable from a comparison of the interrupted curves to the superimposed continuous curves. At 950 and 1000° C, the softening during the 150 second intervals (excluding the first) is large enough that upon reloading the flow stress never reaches the stress for the comparable strain on the continuous test. At lower temperatures where softening is less than 100%, the maximum stress upon reloading exceeds the continuous flow curve in the steady state. The overshoot occurs because of the strain hardening which occurs in the recrystallized grains before the critical strain is reached for dynamic recrystallization to begin. More simply, because the

recrystallized grain size is similar to, or less than, the original grain size, the reloading curve rises towards a peak as the loading curve did at the beginning of deformation and is thus higher than the steady state stress for continuous recrystallization.

The fractional softening which occurred in the above tests compares favourably to that observed in previous work done at this strain rate but at a pass strain of 0.2 (Fig. 4.9). Despite the difference in pass strain, the amount of softening which occurs in the 10 second interruptions at 900 and 950° C is comparable at the same accumulated strain. At 1000° C, the softening after pass strains of 0.3 is much higher than after pass strains of 0.2 indicating that considerable recrystallization is taking place in the former whereas little is taking place in the latter. The softening during the 150 second holds is in all cases much larger indicating that partial or complete recrystallization is occurring.

From the plot of average fractional softening versus $^{1}/_{T}$, the two mechanisms (static recovery and static recrystallization) have different temperature dependences,

i.e., different ΔH values. Straight lines were drawn through the average fractional softening for which static recrystallization was operating. From these lines the calculated ΔH value was approximately 101 Kcal/mole.

Previous work (26,27) figure 3.4 indicates that the precipitation of the niobium is complete within 120 seconds in all cases but 800° C and thus has occurred during the first 150 second interruption (this could partially explain the low static restoration). At 800° C, precipitation continued until approximately 900 seconds. Therefore, precipitation did not interfere with dynamic or static recrystallization after the first interruption except at 800° C.

For the tests conducted at a strain rate of $1.0s^{-1}$ with 10 second pauses at strains of 2.5, the continuous steady state stress is exceeded on each pass (Fig. 4.6). Since the pass strain is greater than the peak strain, a new peak is obtained on each pass. This peak is less than the first one, indicating recrystallization has not gone to completion during the interruption and is proceeding during the subsequent pass.

The amount of softening between passes shown in figure 4.10 indicates the fractional softening was similar at 950 and 1000° C. Examination of the stress-strain curves at strain rate of $1.0s^{-1}$ shows that at 1000° C, the flow stress at the end of each pass approached the flow stress obtained during the continuous tests. This indicates that dynamic recrystallization in the interrupted test has significantly reduced the dislocation density at these conditions. This leaves less driving force for static recrystallization and thus the amount of softening is not significantly different from that at 950° C.

The stress-strain graph (Fig. 4.7) for the interrupted test at 950° C strained at $10s^{-1}$ exhibits the typical peak stress after each interruption. These peaks do not decrease significantly after the second interruption but exceed the steady state flow stress. This reduction in peak stress indicates that recrystallization has not gone to completion during the pause and is proceeding in the subsequent pass. The fractional softening during the pauses (Fig. 4.11) is less than 100% thus confirming the above statement.

CHAPTER 6

Conclusions

The following conclusions were reached regarding the hot working characteristics of a 0.12% C, 0.05% Nb steel:

1) During continuous deformation, dynamic recrystallization occurs at all the strain rates and temperatures. The strain to the peak stress increases with an increase of strain rate or a decrease in temperature.

2) The data obtained in the present trials resulted in a minor revision of the values of the constants in the power law relating the flow stress, strain rate and temperature; ΔH to 104 Kcal/mole and n to 8.6.

3) In the low strain rate tests, principally static recovery occurred during the 10 second pauses or during the first 150 second pause except at 1000° C.

4) Static recrystallization at low strain rates occurs during the 150 second interruptions (after the first) and in the short intervals between strains to steady state at high strain rates.

5) Fractional softening during an interruption rises with increase in a) the duration and temperature of the pause and in b) the amount of accumulated strain energy, i.e., in strain rate, in strain since last recrystallization and in lowered temperature.

6) When the peak flow stress is not reached in the first pass and only recovery acts during an interruption, the flow stress in the second pass returns to the flow curve for a continuous test.

7) When complete recrystallization has occurred, the flow curve in the subsequent pass rises to a peak which overshoots the steady state flow stress.

8) If recrystallization is not complete during a pause, the subsequent pass has a lower peak stress compared to a curve where recrystallization has been allowed to reach completion.

9) When grain growth follows recrystallization the interrupted flow curves fall below the continuous flow curves.

REFERENCES

1) McQueen, H.J., and Jonas, J.J., Treatise on Materials Science and Technology, Vol. 6, Plastic Deformation of Materials, ed. R.J. Arsenault, Academic Press, N.Y., 393-493, 1975

2) Jonas, J.J., Sellars, C.M., and Tegart, W.J. McG., Met. Rev., 14, 1-24, 1967

3) McQueen, H.J., Met. Trans., Vol. 8A, 807-24, 1977

4) McQueen, H.J., Trans. Japan Inst. Metals, 9 Suppl., 170-77, 1968

5) McQueen, H.J., Weiss, H., and Northway, U., Flow Stress and Microstructural Changes in Austenitic Stainless Steel during Hot Torsion, Australia, B.H.P. Melbourne Research Lab., 1973

6) Fulop, S., and McQueen, H.J., "Superalloys Processing", Metals and Ceramics Information Center, Columbus, Ohio, H1-H21, 1972

7) McQueen, H.J., and Bergerson, S., Metal Sci. J., 6, 25-29, 1972

8) McQueen, H.J., Wong, W.A., and Jonas, J.J., Can. J. Physics, 45, 1225-1233, 1967

9) Sellars, C.M., and Tegart, W.J. McG., Int. Met. Rev., 17, 1-24, 1972

10) Jonas, J.J., McQueen, H.J., and Wong, W.A., Iron and Steel Inst., London, 49-59, 1968

11) Jonas, J.J., Pro. 4th Int. Con. of Strength of Metals & Alloys, Nancy, France, Vol. 3, 976-1002, 1976

12) Kivilahti, J.K., Lindroos, V.K., and Lehtinen, B., "High Voltage Electron Microscopy" eds. Swann, P.R., et al, Academic Press, N.Y., 1974

13) Sandstrom, R., and Lagneborg, R., Acta. Met., 23, 387-398, 1975

14) Roberts, W., and Anlblom, B., Proc. 4th Int. Conf. on Strength of Metals and Alloys, Nancy, France, Vol. 1, 400-404, 1976

15) Rossard, C., "A Study of the Hot Plastic Deformation of Steel", Metaux Corros. Inds., 35, 102-15, 140-53, 190-205, 1960

16) Rossard, C., Pro. 3rd Int. Conf. on Strength of Metals and Alloys, Cambridge, England, Vol. 2, 175-203, 1973

17) Luton, M.J., and Sellars, C.M., Acta. Met., 17, 1033-43, 1969

18) Petkovic, R.A., Ph.D. Thesis, McGill University, Montreal, Canada, 1975

19) Petkovic-Djaic, R.A., and Jonas, J.J., J. Iron & Steel Inst., 210, 256-261, 1972

20) Petkovic-Djaic, R.A., and Jonas, J.J., Met. Trans., 4, 621-624, 1973

21) Weiss, H., Gittens, A., Brown, G.G., and Tegart, W.J., McG., "Recrystallization of Steel in the Austenitic Range (MRL 41/1)" BHP Melbourne Research Lab., Australia, 1972

22) Glover, G. and Sellars, C.M., Met. Trans., 3, 2271-2280, 1972

23) Evans, R.W., and Dunstan, G.R., J. Inst., Metals, 99, 4-14, 1971

24) Wong, W.A., McQueen, H.J., and Jonas, J.J., J. Inst. Metals, 95, 129-137, 1967

25) Weiss, I., Ph.D., Thesis, Dept. of Met. Eng., McGill University, Montreal, 1978

26) Jonas, J.J., and Weiss, I., Effect of Precipitation on Recrystallization in Microalloyed Steel, in press

27) Weiss, I., and Jonas, J.J., Interaction between Recrystallization and Precipitation during High Temp. Deformation of HSLA Steels, in press

28) LeBon, A., Rofes-Vernis, J., and Rossard, C., Mém. Sci. Rev. Mét., 70, 577-588, 1973

29) LeBon, A., Rofes-Vernis, J., and Rossard, C., Met. Sci., 9, 36-40, 1975

30) LeBon, A., Rofes-Vernis, J., and Rossard, C., Recristallisation et Précipitation Provoquées par la Déformation à chaud d'Aciers de Construction Soudables microallies au Niobium, Report No. R.E. 331, IRSID, St. Germain-en-Loye, France, 1975

31) LeBon, A., Rofes-Vernis, J., and Rossard, C., "Controlled Processing of HSLA Steels", Paper 6, York Conf., England, 1976

32) Habraken, L.J., Lamberigts, M., and Griday, T., Proc. AIME Seminar on "Hot Deformation of Austenite", Cincinatti, Ohio, 1975

33) Irvine, K.J., Gladman, T., Orr, J., and Pickering, F.B., "Controlled Rolling of Structural Steel", J. Iron Steel Inst., 208, 717-26, 1970

34) Baird, J.D., and Preston, R.R., Some Current Trends in Hot Workability of Mild and Low Alloy Steel, Hot Workability of Steel Symposium, London, Iron Steel Inst., 1969

35) Wilber, G.A., Bell, J.R., Bucher, J.H., and Childs, W.J., Rapid Recrystallization Rates of Austenite at Temperatures of Hot Working, Trans TMS-AIME, 242, 2305-08, 1968

36) Sankar, J., Masters Thesis, Concordia, Univ., Montreal, 1978

37) Fields, D.S., and Backofen, W.A., ASTM Proceedings, 57, 1263-1275, 1975

38) Tegart, W.J. McG., "Elements of Mechanical Metallurgy", McMillan, N.Y. & London, P. 76, 1966

39) Lemmon, D.C., and Sherby, O.D., J. of Mat. 4, 444-456, 1969

40) Rossard, C., Doctorate Thesis, University of Paris, 1960

41) Robbins, J.L., Shepard, O.C., and Sherby, O.D., Trans. A.S.M., 60, 205-216, 1967

42) Dieter, G.E., "Mechanical Metallurgy", McGraw-Hill, N.Y., P. 60, 1961

43) Fulop, S., Cadien, K.C., Luton, M.J., and McQueen, H.J., "A Servo-Controlled Hydraulic Hot Torsion Machine", Faculty of Eng., Concordia University, Montreal, 1974

44) Petkovic, R.A., Luton, M.J., & Jonas, J.J., Can. Met. Quarterly, 14, 137-145, 1975